Supporting Information

Rotational Spectroscopy Probes Lone pair···π-hole Interactions in Hexafluorobenzene-Tertiary Alkylamines Complexes

Dingding Lv,[a] Weixing Li,[a,*] Luca Evangelisti,[b]* Imanol Usabiaga,[c] Camilla Calabrese,[d] Assimo Maris,[e] Sonia Melandri,[e,*] Guanjun Wang,[a] Mingfei Zhou[a,*]

[a]*Department of Chemistry, Collaborative Innovation Center of Chemistry for Energy Materials, Shanghai Key Laboratory of Molecular Catalysis and Innovative Materials, Fudan University, Songhu Rd. 2005, 200438 Shanghai, China.*

[b]*Dipartimento di Chimica "G. Ciamician"- Campus of Ravenna, Università di Bologna, Via Sant'Alberto, I-48123 Ravenna, Italy.*

[c]*Dpto. Química Física, Universidad del País Vasco (UPV/EHU), Barrio Sarrena s/n, 48940 Leioa, Spain.*

[d]*Dpto. Química Física y Química Inorgánica, Facultad de Ciencias – I.U CINQUIMA, Universidad de Valladolid, Paseo de Belén 7, 47011 Valladolid, Spain.*

[e]*Dipartimento di Chimica "G. Ciamician", Università di Bologna, Via Selmi 2, I-40126 Bologna, Italy.*

*Corresponding authors: weixingli@fudan.edu.cn; luca.evangelisti6@unibo.it; sonia.melandri@unibo.it; mfzhou@fudan.edu.cn

Table of Contents

Experimental and Theoretical Procedures

The rotational spectra were recorded with COBRA-type pulsed supersonic-jet Fourier Transform Microwave (FTMW) spectrometer [1-4] and chirped-pulse Fourier Transform Microwave (CP-FTMW) spectrometer.[5-7] The diagram of the CP-FTMW is shown in Scheme S1. Commercial samples of C_6F_6 (bought from Alfa Aesar, purification >99.0%), $N(CH_3)_3$ and NC_7H_{13} (bought from Aldrich, anhydrous 99.9%) were used without further purification.

The C_6F_6-NC_7H_{13} and C_6F_6-$N(CH_3)_3$ were first measured by using the FTMW spectrometer at the University of Bologna. For the measurements of C_6F_6-$N(CH_3)_3$, $N(CH_3)_3$ and C_6F_6 were mixed in a gas tank with He (concentration about 1% for both $N(CH_3)_3$ and C_6F_6 with pressure of 0.3 MPa). For the measurements of C_6F_6-NC_7H_{13}, a gas mixture of C_6F_6 in He (concentration about 1%) was flowed over the solid sample NC_7H_{13} heating at

303 K. The final mixtures were then expanded into the Fabry-Perot cavity through a solenoid valve, which was in the direction along the axis of microwave propagation during the measurement in FTMW spectrometer.

The broadband spectrum of C_6F_6-NC_7H_{13} were measured using a CP-FTMW spectrometer at the Fudan University. NC_7H_{13} was placed in a custom-made reservoir located close to a solenoid pulsed valve at room temperature. The C_6F_6 sample was evaporated into a gas tank and diluted to 0.5% with He. After passing through a 1mm diameter nozzle under a back pressure of 0.3 MPa, the gas mixture expanded into a vacuum chamber, generating a pulsed (8Hz) supersonic jet. After a delay of 860μs, six back-to-back chirped pulses with a duration of 4 μs chirped pulses ranging 2-8GHz are generated by a 25GS/s arbitrary waveform generator. These pulses were then amplified by a 300 Watts traveling wave tube amplifier and broadcasted to the vacuum chamber through the horn antenna. The microwave signal interacted with the molecular beam in mutually perpendicular directions. The subsequent six free induction decay signals of the macroscopic dipole moment of the ensemble of molecules were collected in the horn antenna at the other end, passed through the protection switch, low noise amplifier, and final recorded in the digital oscilloscope. A duration of 40 μs for one FID have been accumulated. The frequency measurement accuracy of the spectrum reached 15 kHz, and the resolution was better than 25 kHz.

We measured the broadband spectrum of C_6F_6-$N(CH_3)_3$ in the frequency range 6-12.5 GHz using the CP-FTMW with a solid-state amplifier (200 W, covering 6-18GHz). The highest frequency of chirped pulses was limited to 12.5GHz due to the sampling rate limitation (25GS/s) of arbitrary waveform generator. The C_6F_6 and $N(CH_3)_3$ samples were vapored into the gas tank and diluted to 0.5% with Ne for both $N(CH_3)_3$ and C_6F_6. A pulsed (7Hz) supersonic jet was generated, and after a delay of about 960 μs, ten back-to-back chirped pulses with a duration of 4 μs ranging from 6 to12.5 GHz frequency were broadcasted into the vacuum chamber. A duration of 20 μs for one FID and a total of 0.4 million FID signal have been accumulated. Other experimental details were the same as the measurement of C_6F_6-NC_7H_{13}.

Quantum chemical calculations, performed at the B3LYP-D4/def2-TZVP level using the Orca 4 program package,[8] predicted the global minimum structures of the complexes of C_6F_6-NH_3, C_6F_6-$N(CH_3)_3$ and C_6F_6-NC_7H_{13} and their sketches are shown in Figure S1. The method and basis set were chosen as they proved to be accurate for the structural characterization of molecular complexes also when dispersion terms are important in shaping the conformational species.

The potential energy functions for the internal rotation of the NH_3, $N(CH_3)_3$ and NC_7H_{13} relative to C_6F_6 are obtained at the B3LYP-D4/def2-TZVP level of theory and the internal rotation coordinate is moved with a step size of 5° while all the other geometrical parameters were freely optimized.

To compute dissociation energies (E_D) accurately, single-point energy calculations at the best-estimated equilibrium geometry of the complex and of the isolated non-interacting fragments were performed. Then, the dissociation energy was evaluated as the difference between the electronic energy of three complexes and those of the isolated monomers, with the BSSE correction taken into account through the counterpoise correction (CP) procedure proposed by Boys and Bernardi.[9] Subsequently, electronic energies were corrected for the harmonic ZPE contribution calculated at the B3LYP-D4/def2-TZVP level. Thus, leading to a ZPE-corrected value for the dissociation energies.

For comparison and to gain a more complete picture of the valence orbitals, a Natural Bond Orbital (NBO)[10] analysis was performed to calculate the populations in the valence p-orbitals. The population of the p orbital derived from NBO are reported in the Table S7.

The distances of weak CH···F hydrogen bond for C_6F_6-$N(CH_3)_3$, and C_6F_6-NC_7H_{13} as listed in Table S8. The values were also compared with C_6F_6-NH_3 and other CH···F hydrogen bond systems.[11-17] The weak hydrogen bond

lengths in the complex of C_6F_6-$N(CH_3)_3$, and C_6F_6-NC_7H_{13} are within the range of reported hydrogen bond lengths.The core-valence bifurcation (CVB) index is a method for examining the hydrogen bond strength proposed by Silvi et al.[18] It is defined by the topological analysis of the electron localization function (ELF).The negative value of CVB index means the strong hydrogen bonds; the CVB index of the medium-strength hydrogen bond is around 0; the more positive value of CVB index means the weaker hydrogen bond. As shown in Table S8, the CH···F hydrogen bonds in C_6F_6-NC_7H_{13} were weaker than C_6F_6-$N(CH_3)_3$ based on the more positive value of CVB index in the C_6F_6-NC_7H_{13}.

The unassigned transition frequencies measured by CP-FTMW and COBRA-FTMW spectrometers for the complexes of C_6F_6-$N(CH_3)_3$, and C_6F_6-NC_7H_{13}, in MHz are listed in Table S9.

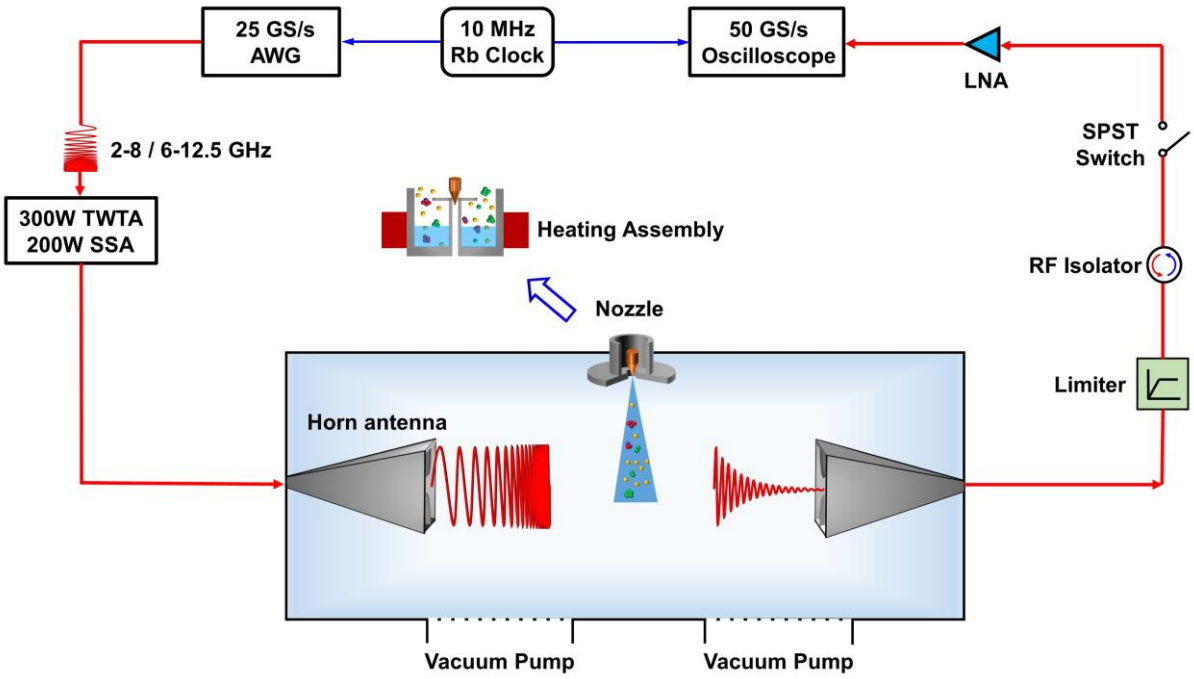

Scheme S1. The diagram of the CP-FTMW spectrometer at Fudan University.

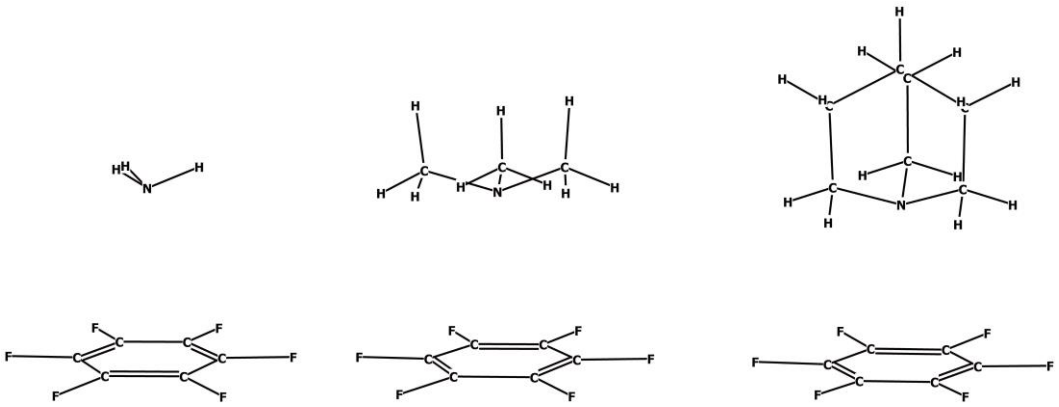

Figure S1. The sketches of the complexes of C_6F_6-NH_3, C_6F_6-$N(CH_3)_3$, and C_6F_6-NC_7H_{13}.

Table S1. Theoretical equilibrium structure (in Å) of C_6F_6-NH_3 in the principal axis system.

	r_e		
	a	b	c
C1	1.311	-0.456	0.334

C2	1.051	0.905	0.334
C3	-0.258	1.360	0.337
C4	-1.306	0.454	0.336
C5	-1.046	-0.907	0.337
C6	0.262	-1.363	0.338
F7	2.058	1.779	0.311
F8	-0.508	2.671	0.320
F9	-2.564	0.894	0.315
F10	-2.053	-1.781	0.319
F11	0.513	-2.673	0.322
F12	2.569	-0.897	0.311
N13	-0.019	0.005	-2.856
H14	0.153	-0.919	-3.237
H15	0.694	0.620	-3.234
H16	-0.910	0.319	-3.225

Table S2. Theoretical equilibrium structure (in Å) of C_6F_6-$N(CH_3)_3$ in the principal axis system.

	r_e		
	a	b	c
C1	1.036	0.844	0.915
C2	-0.247	1.362	0.842
C3	-1.336	0.509	0.765
C4	-1.142	-0.864	0.762
C5	0.141	-1.382	0.835
C6	1.230	-0.529	0.912
F7	-2.188	-1.684	0.660
F8	0.329	-2.702	0.803
F9	2.466	-1.027	0.954
F10	2.085	1.665	0.962
F11	-0.432	2.683	0.817
F12	-2.569	1.008	0.667
N13	0.142	0.026	-2.247
C14	0.751	1.290	-2.617
H15	0.141	2.117	-2.251
H16	1.741	1.372	-2.164
H17	0.865	1.408	-3.709
H18	-1.210	-0.092	-2.760
H19	-1.660	-1.021	-2.409
H20	-1.818	0.739	-2.399
H21	-1.250	-0.088	-3.864
C22	0.967	-1.103	-2.635

H23	1.953	-1.017	-2.177
H24	0.511	-2.032	-2.288
H25	1.103	-1.178	-3.728

Table S3. Theoretical equilibrium structure (in Å) of C_6F_6-NC_7H_{13} in the principal axis system.

	r_e		
	a	b	c
C1	1.386	0.000	-1.773
C2	0.693	-1.200	-1.773
C3	-0.693	-1.200	-1.773
C4	-1.386	0.000	-1.773
C5	-0.693	1.200	-1.773
C6	0.693	1.200	-1.773
F7	-2.719	0.000	-1.743
F8	-1.359	2.355	-1.743
F9	1.359	2.355	-1.743
F10	2.719	0.000	-1.743
F11	1.360	-2.355	-1.743
F12	-1.360	-2.355	-1.743
N13	0.000	0.000	1.265
C14	0.000	1.383	1.752
H15	0.878	1.884	1.341
H16	-0.878	1.884	1.341
C17	1.198	-0.692	1.752
H18	1.192	-1.703	1.341
H19	2.071	-0.181	1.341
C20	-1.198	-0.692	1.752
H21	-2.071	-0.181	1.341
H22	-1.192	-1.703	1.341
C23	0.000	1.441	3.306
H24	0.879	1.975	3.676
H25	-0.879	1.975	3.676
C26	1.248	-0.721	3.306
H27	1.271	-1.748	3.676
H28	2.149	-0.227	3.676
C29	-1.248	-0.721	3.306
H30	-2.149	-0.227	3.676
H31	-1.271	-1.748	3.676
C32	0.000	0.000	3.835
H33	0.000	0.000	4.926

Table S4. Measured transition frequencies of C_6F_6-$N(CH_3)_3$, in MHz.

J'	K_a'	F'	J''	K_a''	F''	ν	$\Delta\nu$
Measured by COBRA-FTMW spectrometer							
8	1	8	7	1	7	7496.9512	0.0001
8	1	7	7	1	6	7496.9583	0.0012
8	1	9	7	1	8	7496.9862	0.0002
8	0	7	7	0	6	7497.1109	0.0008
8	0	8	7	0	7	7497.1281	-0.0029
8	0	9	7	0	8	7497.1448	0.0011
9	1	9	8	1	8	8434.0464	0.0017
9	1	8	8	1	7	8434.0464	-0.0010
9	1	10	8	1	9	8434.0710	0.0003
9	0	8	8	0	7	8434.2256	0.0013
9	0	9	8	0	8	8434.2389	-0.0014
9	0	10	8	0	9	8434.2500	-0.0005
10	1	10	9	1	9	9371.1250	-0.0003
10	1	9	9	1	8	9371.1250	-0.0010
10	1	11	9	1	10	9371.1444	-0.0009
10	0	9	9	0	8	9371.3245	-0.0011
10	0	10	9	0	9	9371.3376	-0.0006
10	0	11	9	0	10	9371.3481	0.0015
11	1	11	10	1	10	10308.1920	-0.0002
11	1	10	10	1	9	10308.1920	0.0001
11	1	12	10	1	11	10308.2067	-0.0013
11	0	10	10	0	9	10308.4137	0.0004
11	0	12	10	0	11	10308.4296	-0.0010
11	0	11	10	0	10	10308.4296	0.0061
12	1	12	11	1	11	11245.2445	-0.0001
12	1	11	11	1	10	11245.2445	0.0008
12	1	13	11	1	12	11245.2580	0.0007
12	0	11	11	0	10	11245.4856	-0.0009
12	0	12	11	0	11	11245.4917	-0.0033
12	0	13	11	0	12	11245.5037	0.0027

Table S5. Measured transition frequencies of C_6F_6-NC_7H_{13}, in MHz.

J'	K_a'	F'	J''	K_a''	F''	ν	$\Delta\nu$
Measured by CP-FTMW spectrometer							
6	0	6	5	0	5	3061.2464	0.0218
6	0	7	5	0	6	3061.2464	0.0020
6	3	6	5	3	5	3060.8583	-0.0098
7	0	7	6	0	6	3571.4302	0.0069
7	1	6	6	1	5	3571.4302	0.0213
8	0	9	7	0	8	4081.6475	0.0159
8	1	9	7	1	8	4081.6475	0.0139
8	2	9	7	2	8	4081.6475	0.0078
8	2	7	7	2	6	4081.6475	0.0220
8	3	7	7	3	6	4081.6475	-0.0105
8	3	9	7	3	8	4081.6475	-0.0025
8	3	8	7	3	7	4081.4535	0.0058
9	0	9	8	0	8	4591.8161	0.0031
9	0	8	8	0	7	4591.8161	0.0183
9	1	9	8	1	8	4591.8161	0.0181
9	1	10	8	1	9	4591.8161	-0.0066
9	1	8	8	1	7	4591.8161	0.0156
9	2	10	8	2	9	4591.8161	-0.0064
9	3	10	8	3	9	4591.8161	-0.0062
9	4	10	8	4	9	4591.8161	-0.0065
9	3	8	8	3	7	4591.8161	-0.0060
9	5	10	8	5	9	4591.8161	-0.0077
9	6	10	8	6	9	4591.8161	-0.0105
9	7	10	8	7	9	4591.8161	-0.0155
10	0	11	9	0	10	5102.0032	-0.0081
10	0	10	9	0	9	5102.0032	-0.0001
10	1	9	9	1	8	5102.0032	0.0118
10	1	11	9	1	10	5102.0032	-0.0065
10	1	10	9	1	9	5102.0032	0.0125
10	2	11	9	2	10	5102.0032	-0.0017
10	3	11	9	3	10	5102.0032	0.0062
10	3	9	9	3	8	5102.0032	0.0101
10	4	11	9	4	10	5102.0032	0.0166
10	5	9	9	5	8	5102.0032	0.0044
10	6	9	9	6	8	5102.0032	-0.0015
10	7	9	9	7	8	5102.0032	-0.0105
10	4	10	9	4	9	5101.7940	-0.0097
11	0	12	10	0	11	5612.2116	0.0148

11	0	11	10	0	10	5612.2116	0.0215
11	1	12	10	1	11	5612.2116	0.0177
12	0	12	11	0	11	6122.3778	0.0049
12	1	13	11	1	12	6122.3778	0.0030
12	1	12	11	1	11	6122.3778	0.0151
12	1	11	11	1	10	6122.3778	0.0159
12	2	13	11	2	12	6122.3778	0.0144
12	5	12	11	5	11	6122.1257	0.0037
12	9	13	11	9	12	6122.1257	0.0090
12	10	11	11	10	10	6122.1257	-0.0161
12	10	13	11	10	12	6122.0495	-0.0204
13	0	14	12	0	13	6632.5786	0.0221
13	3	14	12	3	13	6632.5195	0.0048
13	7	14	12	7	13	6632.3323	-0.0132
13	9	12	12	9	11	6632.2647	-0.0031
Measured by COBRA-FTMW spectrometer							
14	0	15	13	0	14	7142.7287	-0.0012
14	0	14	13	0	13	7142.7287	0.0031
14	0	13	13	0	12	7142.7287	0.0089
14	1	15	13	1	14	7142.7287	0.0043
14	1	14	13	1	13	7142.7148	-0.0013
14	1	13	13	1	12	7142.7148	0.0000
14	2	15	13	2	14	7142.7039	-0.0042
14	2	13	13	2	12	7142.6957	-0.0042
14	2	14	13	2	13	7142.6887	0.0010
14	3	15	13	3	14	7142.6887	0.0074
14	3	13	13	3	12	7142.6757	0.0003
14	3	14	13	3	13	7142.6511	0.0104
14	4	15	13	4	14	7142.6511	0.0065
14	4	13	13	4	12	7142.6511	0.0093
14	5	15	13	5	14	7142.5958	-0.0028
14	5	13	13	5	12	7142.5958	-0.0042
14	4	14	13	4	13	7142.5790	0.0033
14	6	13	13	6	12	7142.5534	0.0026
14	6	15	13	6	14	7142.5534	0.0090
14	6	14	13	6	13	7142.3939	-0.0009
15	0	16	14	0	15	7652.8954	-0.0031
15	0	15	14	0	14	7652.8954	0.0007
15	0	14	14	0	13	7652.8954	0.0057
15	1	16	14	1	15	7652.8954	0.0031
15	1	15	14	1	14	7652.8954	0.0102
15	1	14	14	1	13	7652.8954	0.0115

15	2	16	14	2	15	7652.8716	-0.0024
15	2	14	14	2	13	7652.8716	0.0050
15	2	15	14	2	14	7652.8376	-0.0194
15	3	14	14	3	13	7652.8376	-0.0005
15	3	16	14	3	15	7652.8376	-0.0061
15	3	15	14	3	14	7652.8180	0.0077
15	4	14	14	4	13	7652.8059	0.0069
15	4	16	14	4	15	7652.8059	0.0037
15	4	15	14	4	14	7652.7497	0.0039
15	5	16	14	5	15	7652.7502	0.0000
15	5	14	14	5	13	7652.7502	0.0000
15	6	14	14	6	13	7652.7012	0.0086
15	6	16	14	6	15	7652.6874	-0.0014
15	5	15	14	5	14	7652.6616	-0.0026
15	7	16	14	7	15	7652.6114	-0.0079
15	7	14	14	7	13	7652.6114	-0.0162
15	6	15	14	6	14	7652.5692	0.0026
15	8	16	14	8	15	7652.5346	-0.0085
15	9	14	14	9	13	7652.4714	-0.0100
15	7	15	14	7	14	7652.4584	0.0042
15	9	16	14	9	15	7652.4584	-0.0035
15	8	15	14	8	14	7652.3267	-0.0020
15	11	14	14	11	13	7652.3267	0.0003
15	12	14	14	12	13	7652.2516	0.0003
15	9	15	14	9	14	7652.1812	-0.0104
15	13	14	14	13	13	7652.1686	-0.0126
15	13	16	14	13	15	7652.1291	-0.0019
15	14	16	14	14	15	7652.0424	-0.0170
15	10	15	14	10	14	7652.0333	-0.0117
16	0	17	15	0	16	8163.0589	-0.0030
16	0	16	15	0	15	8163.0589	0.0004
16	0	15	15	0	14	8163.0589	0.0047
16	1	17	15	1	16	8163.0589	0.0039
16	1	15	15	1	14	8163.0349	-0.0128
16	2	17	15	2	16	8163.0349	0.0001
16	2	16	15	2	15	8163.0232	0.0027
16	1	16	15	1	15	8163.0486	-0.0004
16	3	17	15	3	16	8162.9975	-0.0039
16	3	15	15	3	14	8162.9774	-0.0187
16	3	16	15	3	15	8162.9774	0.0039
16	4	15	15	4	14	8162.9573	0.0053
16	4	17	15	4	16	8162.9568	0.0014

16	4	16	15	4	15	8162.9086	0.0000
16	5	17	15	5	16	8162.9046	0.0067
16	5	15	15	5	14	8162.8979	0.0010
16	6	17	15	6	16	8162.8375	0.0077
16	6	15	15	6	14	8162.8375	0.0057
16	5	16	15	5	15	8162.8214	-0.0052
16	7	17	15	7	16	8162.7541	0.0015
16	7	15	15	7	14	8162.7565	-0.0016
16	8	17	15	8	16	8162.6720	0.0042
16	8	15	15	8	14	8162.6720	-0.0053
16	7	16	15	7	15	8162.6157	-0.0004
16	9	15	15	9	14	8162.6002	0.0089
16	9	17	15	9	16	8162.5706	-0.0067
16	8	16	15	8	15	8162.4857	-0.0048
16	10	17	15	10	16	8162.4857	0.0025
16	11	15	15	11	14	8162.4158	0.0032
16	11	17	15	11	16	8162.3846	-0.0032
16	9	16	15	9	15	8162.3535	-0.0003
16	12	15	15	12	14	8162.3190	-0.0057
16	12	17	15	12	16	8162.2947	0.0010
16	13	17	15	13	16	8162.2040	0.0002
16	10	16	15	10	15	8162.2040	-0.0041
16	11	16	15	11	15	8162.0567	0.0011
16	12	16	15	12	15	8161.8991	0.0000
16	13	16	15	13	15	8161.7321	-0.0092
16	13	15	15	13	14	8162.2412	-0.0003
16	14	15	15	14	14	8162.1610	-0.0052
16	14	17	15	14	16	8162.1149	-0.0062
16	15	15	15	15	14	8162.0962	-0.0057
16	15	17	15	15	16	8162.0493	0.0002
16	14	16	15	14	15	8161.5806	-0.0047
16	15	16	15	15	15	8161.4323	-0.0021
17	0	18	16	0	17	8673.2140	-0.0057
17	0	17	16	0	16	8673.2140	-0.0027
17	0	16	16	0	15	8673.2140	0.0011
17	1	18	16	1	17	8673.2140	0.0018
17	1	17	16	1	16	8673.2140	0.0070
17	1	16	16	1	15	8673.2140	0.0083
17	2	18	16	2	17	8673.1885	-0.0016
17	2	17	16	2	16	8673.1885	0.0105
17	2	16	16	2	15	8673.1885	0.0043
17	3	16	16	3	15	8673.1487	-0.0001

17	3	18	16	3	17	8673.1487	-0.0050
17	3	17	16	3	16	8673.1245	-0.0058
17	4	18	16	4	17	8673.0986	-0.0051
17	4	16	16	4	15	8673.0986	-0.0016
17	4	17	16	4	16	8673.0727	0.0084
17	5	16	16	5	15	8673.0443	0.0050
17	5	18	16	5	17	8673.0443	0.0034
17	5	17	16	5	16	8672.9861	0.0050
17	6	18	16	6	17	8672.9663	-0.0002
17	6	16	16	6	15	8672.9663	-0.0010
17	6	17	16	6	16	8672.8815	-0.0003
17	7	18	16	7	17	8672.8815	-0.0006
17	7	16	16	7	15	8672.8810	-0.0046
17	8	18	16	8	17	8672.7997	0.0105
17	8	16	16	8	15	8672.7997	0.0038
17	9	16	16	9	15	8672.7053	0.0051
17	9	18	16	9	17	8672.6991	0.0091
17	10	18	16	10	17	8672.5872	0.0007
17	9	17	16	9	16	8672.5070	0.0039
17	11	16	16	11	15	8672.5070	0.0071
17	11	18	16	11	17	8672.4871	0.0058
17	12	16	16	12	15	8672.4035	0.0029
17	12	18	16	12	17	8672.3825	0.0054
17	10	17	16	10	16	8672.3562	-0.0003
17	13	16	16	13	15	8672.3104	0.0046
17	13	18	16	13	17	8672.2871	0.0101
17	14	16	16	14	15	8672.2198	0.0011
17	11	17	16	11	16	8672.2082	0.0046
17	14	18	16	14	17	8672.1891	0.0049
17	15	16	16	15	15	8672.1535	0.0105
17	15	18	16	15	17	8672.0976	-0.0048
17	12	17	16	12	16	8672.0546	0.0073
17	16	18	16	16	17	8672.0429	0.0077
17	14	17	16	14	16	8671.7473	0.0109
18	3	17	17	3	16	9183.3000	0.0042
18	3	18	17	3	17	9183.3000	0.0196
18	3	19	17	3	18	9183.3000	-0.0004
19	0	20	18	0	19	9693.5067	-0.0104
19	0	19	18	0	18	9693.5067	-0.0079
19	0	18	18	0	17	9693.5067	-0.0049
19	1	20	18	1	19	9693.4977	-0.0108
19	1	19	18	1	18	9693.4977	-0.0067

19	1	18	18	1	17	9693.4977	-0.0055
19	3	18	18	3	17	9693.4333	-0.0034
19	3	19	18	3	18	9693.4333	0.0095
19	3	20	18	3	19	9693.4333	-0.0076
20	0	21	19	0	20	10203.6457	-0.0102
20	0	20	19	0	19	10203.6457	-0.0080
20	0	19	19	0	18	10203.6457	-0.0054
20	1	19	19	1	18	10203.6457	0.0037
20	1	20	19	1	19	10203.6457	0.0025
20	1	21	19	1	20	10203.6457	-0.0011
20	2	19	19	2	18	10203.6193	0.0041
20	2	20	19	2	19	10203.6193	0.0074
20	2	21	19	2	20	10203.6193	-0.0004
20	3	19	19	3	18	10203.5690	-0.0020
20	3	20	19	3	19	10203.5690	0.0089
20	3	21	19	3	20	10203.5690	-0.0059
21	0	22	20	0	21	10713.7763	-0.0115
21	0	21	20	0	20	10713.7763	-0.0095
21	0	20	20	0	19	10713.7763	-0.0071
21	1	20	20	1	19	10713.7763	0.0025
21	1	21	20	1	20	10713.7763	0.0014
21	1	22	20	1	21	10713.7763	-0.0019
21	3	20	20	3	19	10713.6869	-0.0115
21	3	21	20	3	20	10713.6869	-0.0022
21	3	22	20	3	21	10713.6869	-0.0151

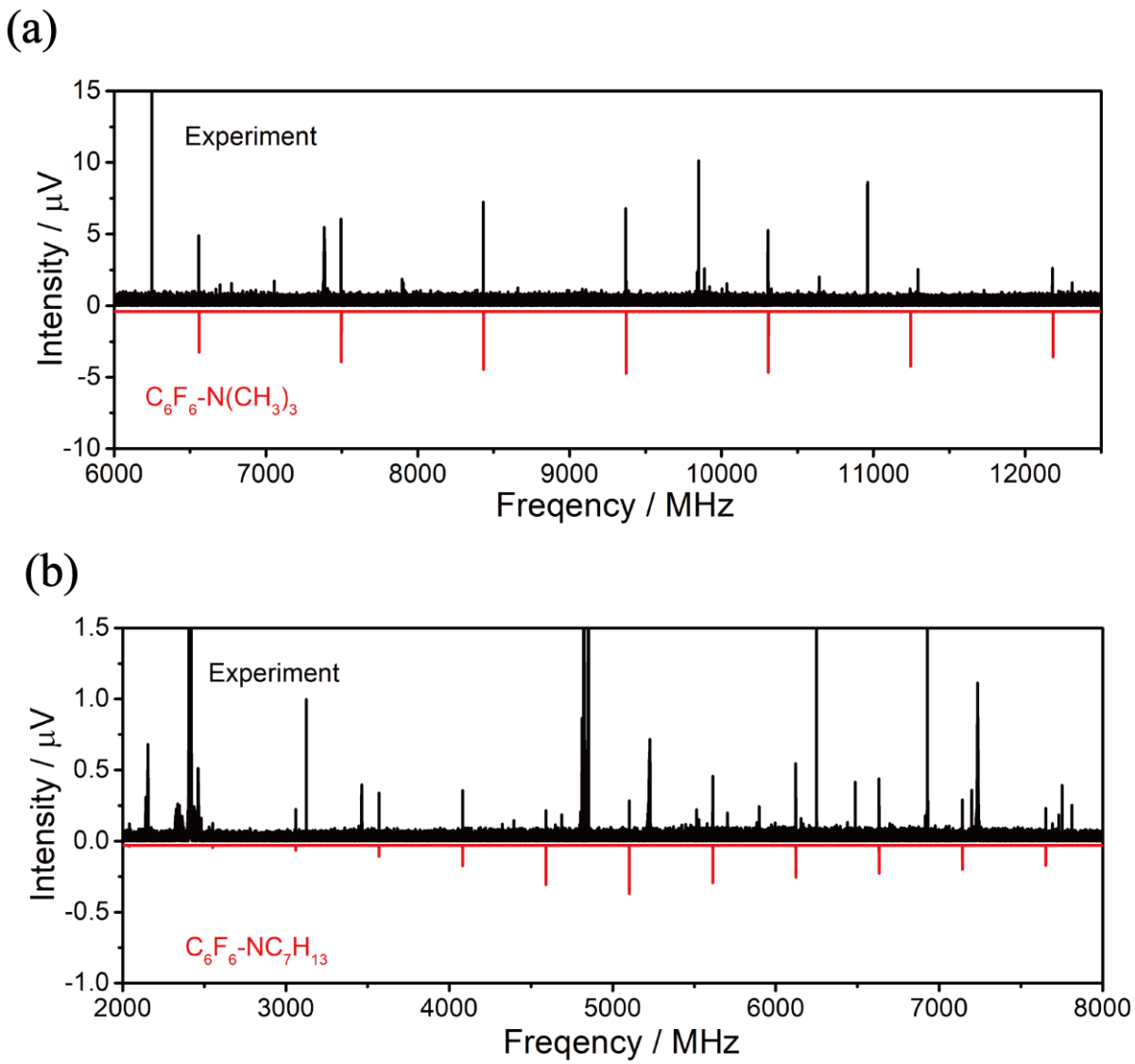

Figure S2. Comparison between the experimental broadband (black) and theoretical (red, T=*1*K) spectra of C_6F_6-$N(CH_3)_3$, and C_6F_6-NC_7H_{13}.

Table S6. SAPT2+3(CCD)/aug-cc-pVDZ analysis for the complexes of NH_3, $N(CH_3)_3$ and NC_7H_{13} with C_6F_6, all values in kJ mol^{-1}.

Energies	Electrostatic	Induction	Dispersion	Exchange	Total
$C_6F_6\cdots NH_3$	-16.0 (49%)[a]	-3.1 (10%)	-13.4 (41%)	17.6	-14.9
$C_6F_6\cdots N(CH_3)_3$	-20.7 (35%)	-4.3 (7%)	-33.6 (57%)	32.5	-26.0
$C_6F_6\cdots NC_7H_{13}$	-27.4 (38%)	-5.4 (8%)	-38.4 (54%)	39.2	-32.0

[a] The percentage of total attractive energy (the sum of Electrostatic, induction and dispersion interaction).

Table S7. Valence p-orbital population anisotropy from the NBO result of the complexes of C_6F_6-NH_3, C_6F_6-$N(CH_3)_3$, and C_6F_6-NC_7H_{13}.

	P_{xx}	P_{yy}	P_{zz}	Sum	P_{ave}	ΔP_{xx}	ΔP_{yy}	ΔP_{zz}
C_6F_6-NH_3	1.353	1.353	1.832	4.538	1.513	-0.160	-0.160	0.319
C_6F_6-$N(CH_3)_3$	1.193	1.193	1.744	4.130	1.377	-0.183	-0.183	0.367
C_6F_6-$C_7H_{13}N$	1.175	1.175	1.742	4.092	1.364	-0.189	-0.189	0.378

NH_3	1.343	1.343	1.842	4.528	1.509	-0.166	-0.166	0.332
$N(CH_3)_3$	1.184	1.184	1.739	4.106	1.369	-0.185	-0.185	0.370
$C_7H_{13}N$	1.169	1.169	1.736	4.074	1.358	-0.189	-0.189	0.378

Table S8. Distances ($r_{CH\cdots F}$) and bonding strength (CVB index) of the weak CH···F hydrogen bond for C_6F_6-NH_3, C_6F_6-$N(CH_3)_3$, and C_6F_6-NC_7H_{13} in the minimum state and the distances of the CH···F ($r_{CH\cdots F\text{-}TS}$) in the transitions state.

	$r_{CH\cdots F}$ / Å	$r_{CH\cdots F\text{-}TS}$ / Å	CVB index
C_6F_6-NH_3	4.041[a] /3.968[b]	4.051[b]	-
C_6F_6-$N(CH_3)_3$	3.193[a]/3.170[b]	3.329[b]	0.0847
C_6F_6-NC_7H_{13}	3.169[a]/3.157[b]	3.322[b]	0.0852
$(CH_2F_2)_n$	2.476~3.549[11-13]		0.0897~0.1000
CH_3F-HCF_3	2.43(1)~3.05(2)[14]/2.369~3.029[b]		0.0893~0.0899
Pyridine-HCF_3	2.700(7)[15]/2.802[b]		0.0871
C_2H_4O-HCF_3	2.74(1) [16]/2.753[b]		0.0837
C_2H_4S-HCF_3	2.66(3)[17]/2.635[b]		0.0794

[a] From the r_0 structures.

[b] Calculated at the B3LYP-D4/def2-TZVP level.

Table S9. List of the unassigned transition frequencies measured by CP-FTMW and COBRA-FTMW spectrometers for the complexes of C_6F_6-$N(CH_3)_3$, and C_6F_6-NC_7H_{13}, in MHz.

C_6F_6-$N(CH_3)_3$		C_6F_6-NC_7H_{13},	
CP-FTMW	COBRA-FTMW	CP-FTMW	COBRA-FTMW
6557.7318	7493.8164	2040.6079	7141.7409
6557.9394	7493.8916	2040.7456	7141.7610
7494.5459	7493.9732	2040.8500	7141.7731
7494.7665	7494.0226	2550.6706	7141.8170
7497.1518	7494.4449	2550.7786	7141.8442
8431.3242	7494.5270	2551.0610	7142.4591
8431.5716	7494.5475	3060.7798	7651.7771
8434.2505	7494.5947	3060.9159	7651.8216
9367.9969	7494.7705	3061.0515	7651.8647
9368.0948	7494.8345	3061.1203	7651.9494
9368.3596	7495.0430	3570.9701	7651.9572
9371.3421	7495.1238	3571.0425	7652.4378
10304.8018	7495.1797	3571.2701	8161.7893
10304.8654	7495.2322	4081.1000	8161.8154
10305.1439	7495.9685	4081.1870	8161.9203
10308.2224	7496.0082	4591.1977	8161.9574
10308.4283	7496.0488	4591.3129	8162.0123
11241.5572	8430.6202	4591.6054	8162.8314

11243.9864	8430.6812	5101.3359	8671.7689
12178.1691	8430.7063	5101.4443	8671.7689
12178.2323	8430.7722	5611.4497	8671.9619
12178.3549	8430.7969	5611.5877	8672.5796
12178.6723	8431.2558	5611.9461	9182.3428
12178.6902	8431.3321	6121.5578	9182.3963
	8431.4377	6121.7195	9182.4466
	8431.5544	6631.6334	9182.5001
	8431.8705	6631.6825	9182.8067
	8431.9205	6631.8384	9182.9286
	8432.0109	6632.1881	9183.2739
	8432.8861	7141.7361	9183.3156
	8432.9105	7141.7956	9183.3294
	8433.0900	7141.9535	9693.0463
	8433.2407	7651.8328	9693.1187
	9367.9870	7651.8984	9693.2302
	9368.0122		9693.2870
	9368.0487		10713.5609
	9368.0946		
	9368.1890		
	9368.3275		
	9368.3593		
	9369.1411		
	9369.1927		
	9370.1014		
	9370.2060		
	10303.7651		
	10303.9297		
	10304.0516		
	10304.7869		
	10304.8627		
	10305.5234		
	10305.7480		
	10305.8844		
	10307.6665		

References

(1) Grabow, J.-U.; Stahl, W.; Dreizler, H. A Multioctave Coaxially Oriented Beam-Resonator Arrangement Fourier-Transform Microwave Spectrometer. *Rev. Sci. Instrum.* **1996**, *67*, 4072-4084.

(2) Balle, T. J.; Flygare, W. H. Fabry–Perot Cavity Pulsed Fourier Transform Microwave Spectrometer with a Pulsed Nozzle Particle Source. *Rev. Sci. Instrum.* **1981**, *52*, 33-45.

(3) Caminati, W.; Millemaggi, A.; Alonso, J. L.; Lesarri, A.; López, J. C.; Mata, S. Molecular Beam Fourier Transform Microwave Spectrum of the Dimethylether–Xenon Complex: Tunnelling Splitting and 131Xe Quadrupole Coupling Constants. *Chem. Phys. Lett.* **2004**, *392*, 1-6.

(4) Caminati, W.; Evangelisti, L.; Feng, G.; Giuliano, B. M.; Gou, Q.; Melandri, S.; Grabow, J.-U. On the Cl···C Halogen Bond: A Rotational Study of CF_3Cl-CO. *Phys. Chem. Chem. Phys.* **2016**, *18*, 17851-17855.

(5) Brown, G. G.; Dian, B. C.; Douglass, K. O.; Geyer, S. M.; Shipman, S. T.; Pate, B. H. A Broadband Fourier Transform Microwave Spectrometer Based on Chirped Pulse Excitation. *Rev. Sci. Instrum.* **2008**, *79*, 53103-53103.

(6) Neill, J. L.; Shipman, S. T.; Alvarez-Valtierra, L.; Lesarri, A.; Kisiel, Z.; Pate, B. H. Rotational Spectroscopy of Iodobenzene and Iodobenzene–Neon with a Direct Digital 2–8 Ghz Chirped-Pulse Fourier Transform Microwave Spectrometer. *J. Mol. Spectrosc.* **2011**, *269*, 21-29.

(7) Schmitz, D.; Shubert, V. A.; Betz, T.; Schnell, M. Multi-Resonance Effects within a Single Chirp in Broadband Rotational Spectroscopy: The Rapid Adiabatic Passage Regime for Benzonitrile. *J. Mol. Spectrosc.* **2012**, *280*, 77-84.

(8) Neese, F.; Wennmohs, F.; Becker, U.; Riplinger, C. The Orca Quantum Chemistry Program Package. *J. Chem. Phys.* **2020**, *152*, 224108.

(9) Boys, S. F.; Bernardi, F. The Calculation of Small Molecular Interactions by the Differences of Separate Total Energies. Some Procedures with Reduced Errors. *Mol. Phys.* **1970**, *19*, 553-566.

(10) Glendening, E. D.; Reed, A. E.; Carpenter, J. E.; Weinhold, F. NBO Version 3.1; Gaussian Inc.: Pittsburgh, 2003.

(11) Blanco, S.; Melandri, S.; Ottaviani, P.; Caminati, W. Shapes and Noncovalent Interactions of Oligomers: The Rotational Spectrum of the Difluoromethane Trimer. *J. Am. Chem. Soc.* **2007**, *129*, 2700-2703.

(12) Caminati, W.; Melandri, S.; Moreschini, P.; Favero, P. G. The C-F···H-C "Anti-Hydrogen Bond" in the Gas Phase: Microwave Structure of the Difluoromethane Dimer. *Angew. Chem. Int. Ed.* **1999**, *38*, 2924-2925.

(13) Feng, G.; Evangelisti, L.; Cacelli, I.; Carbonaro, L.; Prampolini, G.; Caminati, W. Oligomers Based on Weak Hydrogen Bond Networks: A Rotational Study of the Tetramer of Difluoromethane. *Chem. Commun.* **2014**, *50*, 171-173.

(14) Caminati, W.; López, J. C.; Alonso, J. L.; Grabow, J. U. Weak CH···F Bridges and Internal Dynamics in the CH3F-CHF3 Molecular Complex. *Angew. Chem.* **2005**, *117*, 3908-3912.

(15) Favero, L. B.; Giuliano, B. M.; Maris, A.; Melandri, S.; Ottaviani, P.; Velino, B.; Caminati, W. Features of the C-H · · · N Weak Hydrogen Bond and Internal Dynamics in Pyridine–CHF3. *Eur. J. Chem.* **2010**, *16*, 1761-1764.

(16) Alonso, J. L.; Antolínez, S.; Blanco, S.; Lesarri, A.; López, J. C.; Caminati, W. Weak C-H···O and C-H···F-C Hydrogen Bonds in the Oxirane-Trifluoromethane Dimer. *J. Am. Chem. Soc.* **2004**, *126*, 3244-3249.

(17) Cocinero, E. J.; Sánchez, R.; Blanco, S.; Lesarri, A.; López, J. C.; Alonso, J. L. Weak Hydrogen Bonds C–H··· S and C–H···F–C in the Thiirane–Trifluoromethane Dimer. *Chem. Phys. Lett.* **2005**, *402*, 4-10.

(18) Fuster, F.; Silvi, B. Does the Topological Approach Characterize the Hydrogen Bond? *Theor. Chem. Acc.* **2000**, *104*, 13-21.